Supplementary information

Layer 5 myelination gates corticothalamic coincidence detection

Nora Jamann[1,2,5], Jorrit S. Montijn[3], Naomi Petersen[1], Roeland Lokhorst[4], Daan van den Burg[1], Maayke Balemans[1], Stan L.W. Driessens[1,6], J. Alexander Heimel[3] and Maarten H.P. Kole[1,2,*]

Supplementary Figures

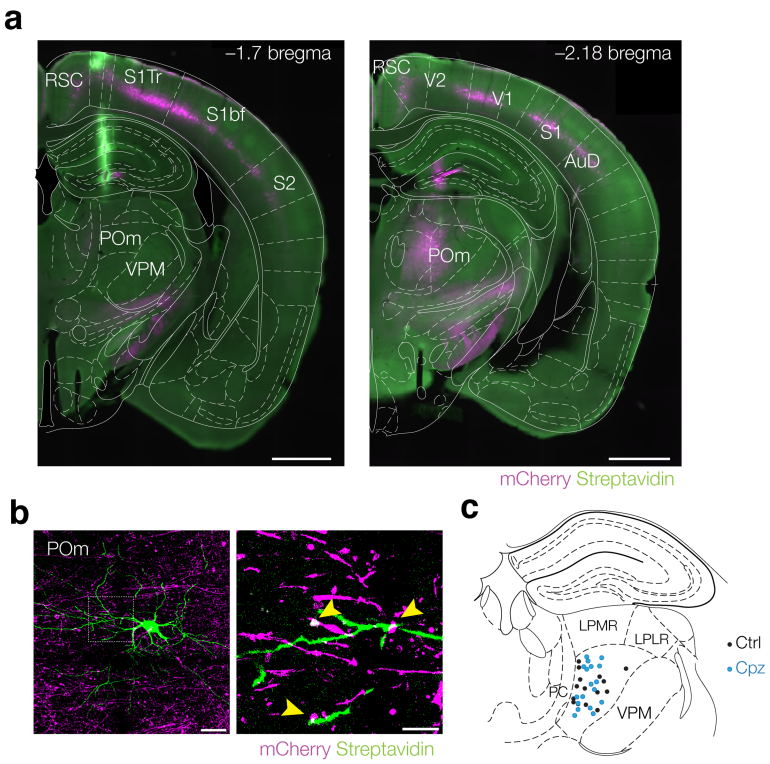

Supplementary Fig. 1 Reconstruction of recording locations in the POm
a Confocal images of a coronal brain section with pipette tracks from biocytin spill in the extracellular solution (Streptavadin, green) and mCherry$^+$ fluorescence (magenta) overlaid with a mouse coronal atlas. Scale bar, 1 mm.
b Confocal image of an opto-tagged juxtacellularly recorded POm neuron filled with biocytin (streptavadin, green) surrounded by mCherry$^+$ L5 axons (magenta) and putative presynaptic terminals (yellow arrows). Scale bars, 30 µm (*left*), 10 µm (*right*).
c Overview of reconstructed locations of recovered neurons based on extrapolation of pipette tracks and noted *z*-depths of recording. VPM, ventral posteromedial thalamic nucleus; LPMR, lateral posterior thalamic nucleus, laterorostral part; LPLR, lateral posterior thalamic nucleus, mediorostral part; PC, paracentral thalamic nucleus. n = 14 neurons, N = 14 mice (Ctrl), n = 18 neurons, N = 13 mice (Cpz).

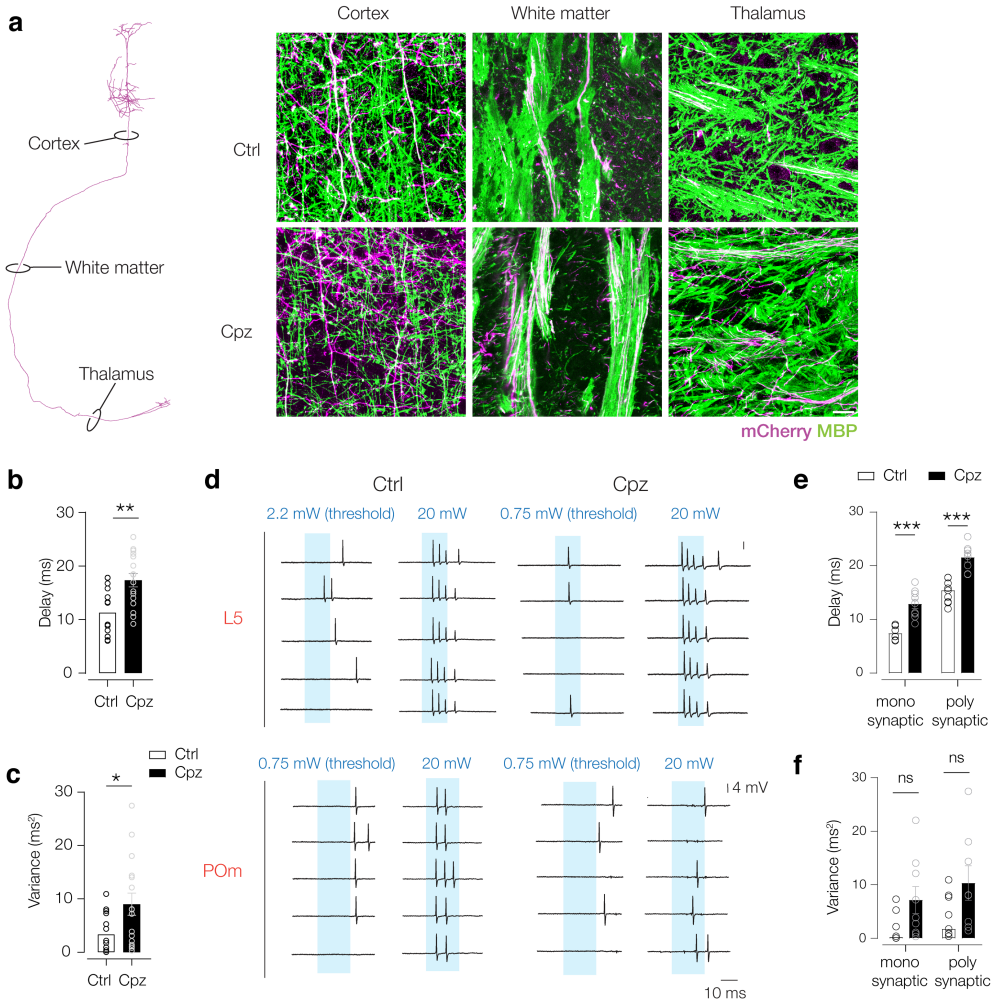

Supplementary Fig. 2 Cortical demyelination delays L5 – POm spiking independent of light output power or connection type

a L5–POm example neuron and confocal images of myelination (MBP, green) in regions that mCherry^{+} axons (magenta) are traveling through in Ctrl and Cpz mice.

b Increased delay at 25 mW of Cpz (black) vs Ctrl (white) neurons. Unpaired t-test **P = 0.0013.

c Increased variance at 25 mW of Cpz (black) vs Ctrl (white) neurons. Unpaired t-test **P = 0.0022. For b, c; n = 15 neurons, N = 11 mice (Ctrl), n = 16 neurons, N = 10 mice (Cpz).

d 5 consecutive example trials of a Ctrl and Cpz neuron in L5 and POm respectively, recorded at low light power (threshold for spiking, left) and high light power (20 mW, right). Note the increased spike numbers, but lower delay and variance at high light power.

e Increased delay of both putative monosynaptic and polysynaptic connections in Cpz (black) vs Ctrl (white) neurons. 2-way ANOVA P < 0.0001 connection type & treatment, P = 0.46 interaction, Šídák's multiple comparisons ***P < 0.001.

f Significant increase in variance of putative monosynaptic and polysynaptic connections for Cpz neurons (treatment effect) does not depend on connection type. 2-way ANOVA *P = 0.027 treatment, P = 0.24 connection type, P = 0.799 interaction, Šídák's multiple comparison P > 0.05. For e, f; n = 17 neurons, N = 11 mice (Ctrl), n = 17 neurons, N = 10 mice (Cpz).

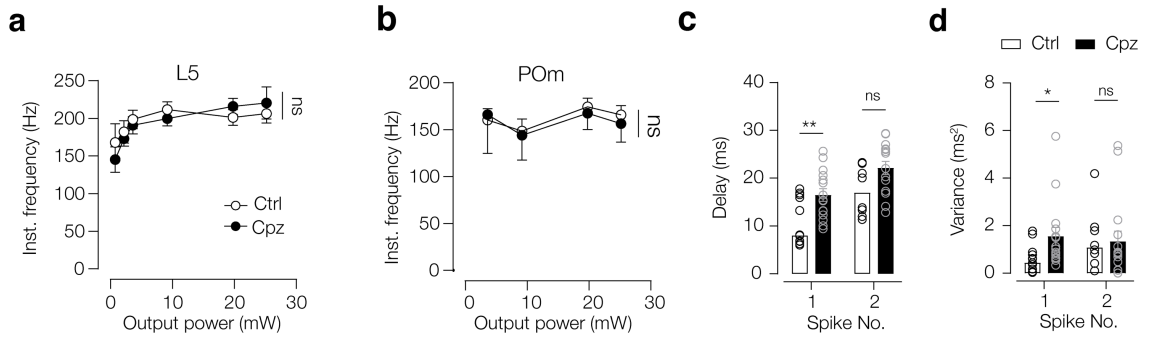

Supplementary Fig. 3 Burst frequencies in L5 and POm are not affected by demyelination

a Instantaneous frequency of light-evoked bursting in L5 pyramidal neurons was not changed in demyelination. 2-way ANOVA P = 0.66 treatment, P = 0.006 output power, P = 0.79 interaction. Šídák's multiple comparisons P > 0.05 for all comparisons. n = 8 neurons, N = 6 mice (Ctrl), n = 5 neurons, N = 4 mice (Cpz).

b Instantaneous frequency of bursting in POm neurons was not changed between treatment groups. 2-way ANOVA P = 0.79 treatment, P = 0.58 output power, P = 0.99 interaction. Šídák's multiple comparisons P > 0.05 for all comparisons. n = 13 neurons, N = 11 mice (Ctrl), n = 12 neurons, N = 8 mice (Cpz).

c First spike in a burst was significantly delayed in Cpz neurons. 2-way ANOVA P = 0.0006 treatment, P = 0.0001 spike nr., P = 0.71 interaction, Šídák's multiple comparisons **P = 0.0065.

d Variance is specifically increased for the first spike in a burst in Cpz neurons. Kruskal-Wallis test P = 0.0595, Dunn's multiple comparisons *P = 0.0483 Ctrl vs Cpz (spike nr. 1), P > 0.05 other comparisons. For c, d**;** n = 13 neurons, N = 9 mice (Ctrl), n = 15 neurons, N = 9 mice (Cpz).

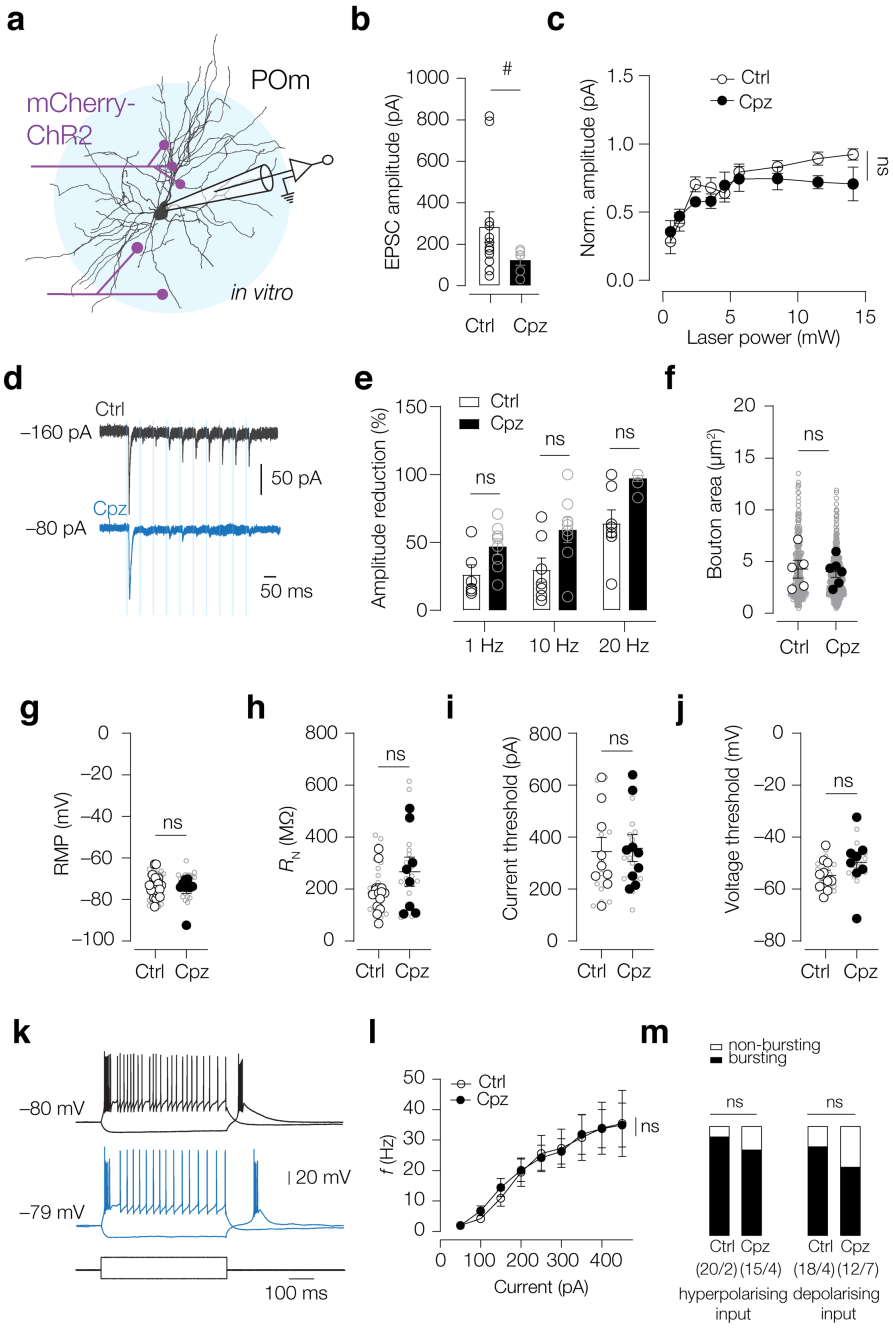

Supplementary Fig. 4. *In vitro* evoked responses of L5–POm boutons as well as intrinsic firing properties were not changed after demyelination

a 3D reconstruction of a neuron recorded in whole-cell configuration *in vitro* and filled with biocytin for post-hoc localization. Neurons were stimulated with a laser (470 nm) above the soma and responses were recorded in voltage clamp.

b Maximum amplitude of evoked EPSCs during stimulation with a single stimulus (10 ms) was not significantly changed. Mann-Whitney test $^{\#}P = 0.0668$, n = 12 neurons, N = 7 mice (Ctrl), n = 6 neurons, N = 4 mice (Cpz).

c Normalized (to maximum response) amplitude in relation to the output light power was not different between groups. 2-way ANOVA $P < 0.0001$ intensity, $P = 0.063$ treatment, $P = 0.45$ interaction, Šídák's multiple comparisons $P > 0.05$ for all comparisons. n = 11 neurons, N = 8 mice (Ctrl), n = 6 neurons, N = 4 mice (Cpz).

d Optical stimulation at 20 Hz (10 x 3 ms) evoked strong postsynaptic depression.

e Relative amplitude reduction of EPSCs at different stimulation frequencies, stimulation at 5 mW output power. No significant changes between Ctrl and Cpz neurons were observed. Facilitating cells were not included in the analysis. Kruskal-Wallis test P = 0.0002, Dunn's multiple comparisons P > 0.05 for all comparisons.
f Bouton area of Ctrl and Cpz L5 axon boutons in POm was the same. Nested t-test P = 0.81, n = 291 boutons, N = 5 mice (Ctrl), n = 514 boutons, n = 6 mice (Cpz).
g Resting membrane potential (RMP) at *I* = 0 of Ctrl and Cpz POm neurons was not significantly different. Liquid junction potential (LJP) of –13 mV was corrected for. Mann-Whitney test P = 0.87. n = 41 neurons, N = 25 mice (Ctrl), n = 23 neurons, N = 9 mice (Cpz).
h Input resistance (R_N) of Ctrl and Cpz POm neurons was not significantly different. Nested t-test P = 0.13. n = 22 neurons, N = 15 mice (Ctrl), n = 20 neurons, N = 8 mice (Cpz).
i Current threshold for single AP generation of Ctrl and Cpz POm neurons was not significantly different. Nested t-test P = 0.91. n = 16 neurons (Ctrl), n = 20 neurons (Cpz), N = 9 mice (Ctrl & Cpz).
j Voltage threshold for single AP generation of Ctrl and Cpz POm neurons was not significantly different. LJP was corrected for. Nested t-test P = 0.91. n = 17 neurons, N = 10 mice (Ctrl), n = 16 neurons, N = 8 (Cpz).
k Current injection responses of a Ctrl (black) and Cpz (blue) neuron. Note the hyperpolarization-evoked rebound bursting as well as the low-current input depolarization evoked bursts. –100 pA and +250 pA current injections respectively.
l Input-frequency relationship was unchanged between Ctrl and Cpz neurons. Average frequency was determined over the entire 500 ms current step. 2-way ANOVA P = 0.83 treatment, P < 0.0001 input current, P > 0.99 interaction. Šídák's multiple comparisons P > 0.99 for all comparisons. n = 15 neurons, N = 11 mice (Ctrl), n = 13 neurons, N = 7 mice (Cpz).
m *Left*: Fraction of hyperpolarization evoked burst-firing neurons. n indicated in figure. Fischer's exact test P = 0.39. *Right***:** Fraction of depolarization evoked burst-firing neurons. n indicated in figure. Fischer's exact test P = 0.29. N = 14 mice (Ctrl), N = 8 (Cpz).

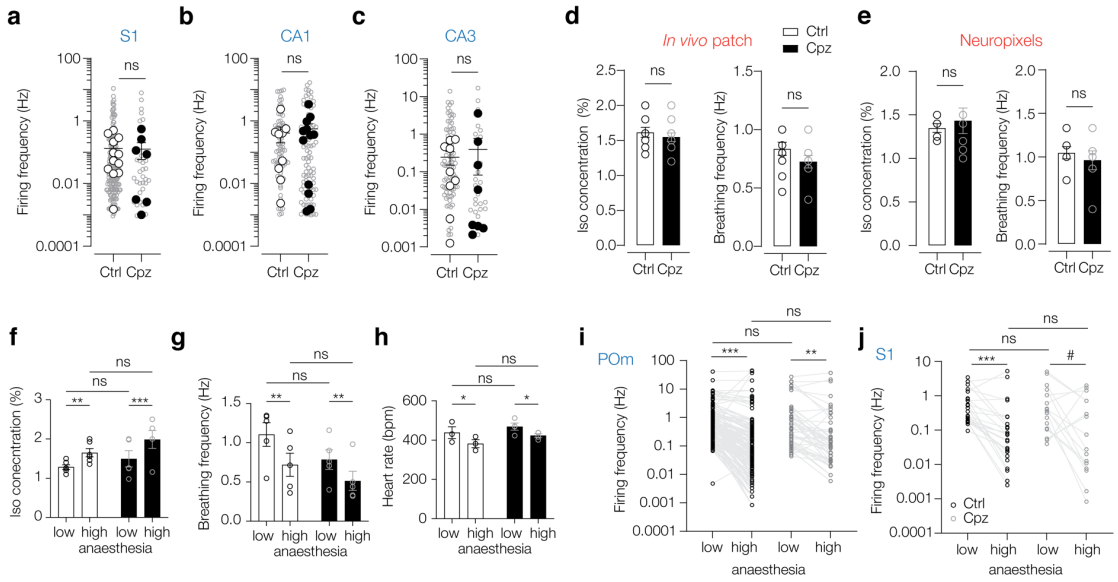

Supplementary Fig. 5 Spontaneous firing frequencies depend on anesthesia depth but not treatment

a Average firing frequency of single units in S1 was unchanged. Mann-Whitney test (over animal means) P = 0.71. n = 192 neurons, N = 12 mice (Ctrl), n = 34 neurons, N = 7 mice (Cpz).

b Average firing frequency of single units in CA1 was unchanged. Mann-Whitney test (over animal means) P = 0.97. n = 77 neurons, N = 9 mice (Ctrl). n = 84 neurons, N = 12 mice (Cpz).

c Average firing frequency of single units in CA3 was unchanged. Mann-Whitney test (over animal means) P = 0.42. n = 83 neurons, N = 9 mice (Ctrl), n = 26 neurons, N = 8 mice (Cpz).

d *Left*: Isoflurane concentration used to anesthetize the *in vivo* patched mice. Unpaired t-test P = 0.48. N = 13 (Ctrl), N = 11 (Cpz). *Right*: Breathing frequency. t-test P = 0.18. N = 11 (Ctrl), N = 9 (Cpz).

e *Left*: Isoflurane concentration used to anaesthetize the Neuropixels mice. Mann-Whitney test P = 0.986. N = 7 mice (Ctrl), N = 9 mice (Cpz). *Right*: Breathing frequency. t-test P = 0.52. N = 7 mice (Ctrl & Cpz).

f Iso % for low and high anesthesia recordings. Paired 2-way ANOVA P = 0.0001 anaesthesia, P = 0.2 treatment, P = 0.0013 neuron. Uncorrected Fischer's LSD **P = 0.003, ***P = 0.0008, P > 0.05. N = 6 mice (Ctrl), N = 5 (Cpz).

g Breathing rate for low and high anesthesia recordings. Paired 2-way ANOVA P = 0.0004 anaesthesia, P = 0.19 treatment, P = 0.0013 neuron. Uncorrected Fischer's LSD **P < 0.01, P > 0.05. N = 5 mice (Ctrl & Cpz)

h Heart rate for low and high anesthesia recordings. Paired 2-way ANOVA P = 0.0084 anaesthesia, P = 0.21 treatment, P = 0.07 cell. Uncorrected Fischer's LSD P > 0.05 for all comparisons. N = 3 mice (Ctrl), N = 4 mice (Cpz).

i Firing frequency for POm neurons was significantly higher at low anesthesia levels for both Ctrl and Cpz mice. Kruskal-Wallis P < 0.0001, Dunn's multiple comparisons ***P < 0.0001 Ctrl high vs low, **P < 0.0032 Cpz high vs low, n = 160 single units, N = 4 mice (Ctrl), n = 49 single units, N = 2 mice (Cpz).

j Firing frequency for L5 neurons was higher at low anesthesia levels for Ctrl mice. A similar trend was observed for Cpz mice. Kruskal-Wallis P = 0.0002, Dunn's multiple comparisons **P = 0.006 Ctrl high vs low, #P = 0.08 Cpz high vs low. n = 27 single units, N = 5 mice (Ctrl), n = 17 single units, N = 3 mice (Cpz).

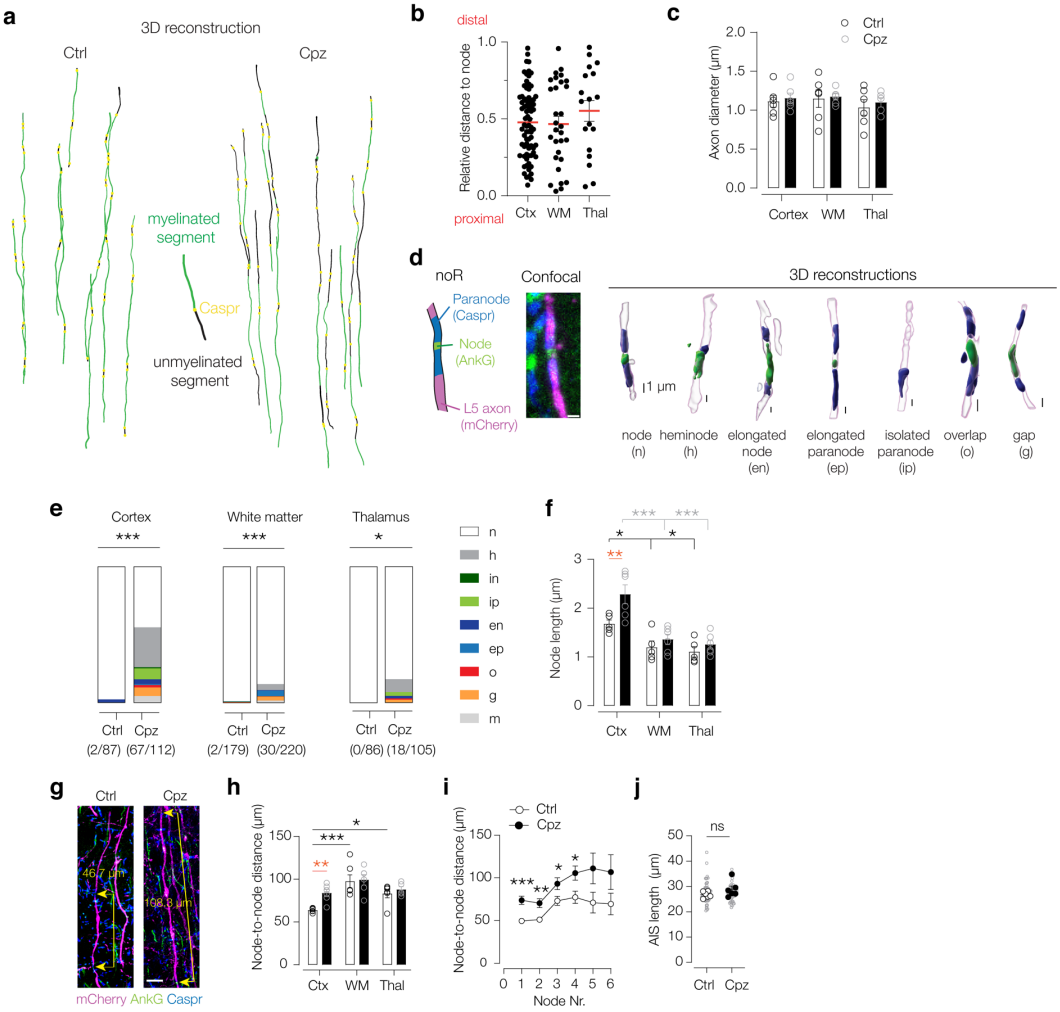

Supplementary Fig. 6 Remodeling of axonal microdomains after demyelination

a 3D Neurolucida reconstructions depicting the highly heterogeneous pattern of cortical demyelination of L5 axons after 6 weeks Cpz treatment.

b No preference for location of axonal spheroids within an internode (proximal or distal). One-way ANOVA P = 0.45. n = 76 swellings in cortex (Ctx), n = 30 white matter (WM), n = 18 thalamus (Thal), N = 8 mice.

c No change in average axon diameter after demyelination. Two-way ANOVA P = 0.51 treatment, P = 0.52 region, P = 0.97 interaction. Tukey's multiple comparisons test P > 0.05 for all comparisons. n = 495 axons, N = 6 mice (Ctrl), n = 445 axons, N = 6 mice (Cpz).

d 3D reconstruction with Imaris software of confocal images of noR depicting a variety of different aberrant morphologies after demyelination, including heminodes, isolated compartments, gaps and overlaps between node and paranode. Scale bars, 1 µm.

e Aberrant node morphologies can be found in all three regions after demyelination, most prominently in the cortex (~55%) but to a lesser extent in WM (~13%) and thalamus (~17%). There were only a few aberrant nodes in the Ctrl case. Chi^2 test ***P < 0.0001 (Ctx), ***P< 0.0008 (WM), *P = 0.012 thalamus. Number of neurons indicated in figure.

f Node length was significantly increased in the cortex after Cpz. 2-way ANOVA P = 0.0064 treatment, P < 0.0001 region, P = 0.14 interaction, Tukey's multiple comparisons **P < 0.0022 Ctx Ctrl vs Cpz, *P < 0.05 Ctrl Ctx vs WM & Thal, ***P < 0.0001 Cpz Ctx vs WM, Thal. n = 81, 192, 67 nodes (Ctrl Ctx, WM, Thal), n = 83, 244, 96 nodes (Cpz Ctx, WM, Thal).

e, f N = 5 mice (Ctrl), N = 6 mice (Cpz).

g Confocal image of node-to-node distance reconstructed by tracing individual axons and denoting locations of AnkG+ nodes.
h Node-to-node distance was significantly increased in the cortex of Cpz mice. 2-way ANOVA P = 0.04 treatment, P = 0.0001 region, P = 0.17 interaction. Tukey's multiple comparisons **P = 0.0083 Ctx Ctrl vs Cpz. ***P = 0.0001 Ctrl Ctx vs WM, *P = 0.027 Ctrl Ctx vs Thal. n = 717 internodes (Ctrl), n = 558 internodes (Cpz).
i Node-to-node distances were increasingly longer with increasing distance from the soma in both Ctrl and Cpz axons. However, starting from the first internode, Cpz nodes are significantly further away. 2-way ANOVA P < 0.0001 node-nr., P < 0.0001 treatment, P = 0.79 interaction. Šídák's multiple comparisons * P < 0.04, **P = 0.009, ***P = 0.0001. n = 74 internodes (Ctrl), n = 56 (Cpz).
j AIS length was unchanged between Ctrl and Cpz neurons. Nested t-test P = 0.22. n = 87 AIS (Ctrl), n = 62 AIS (Cpz).
h, i, j N = 6 mice (Ctrl & Cpz).

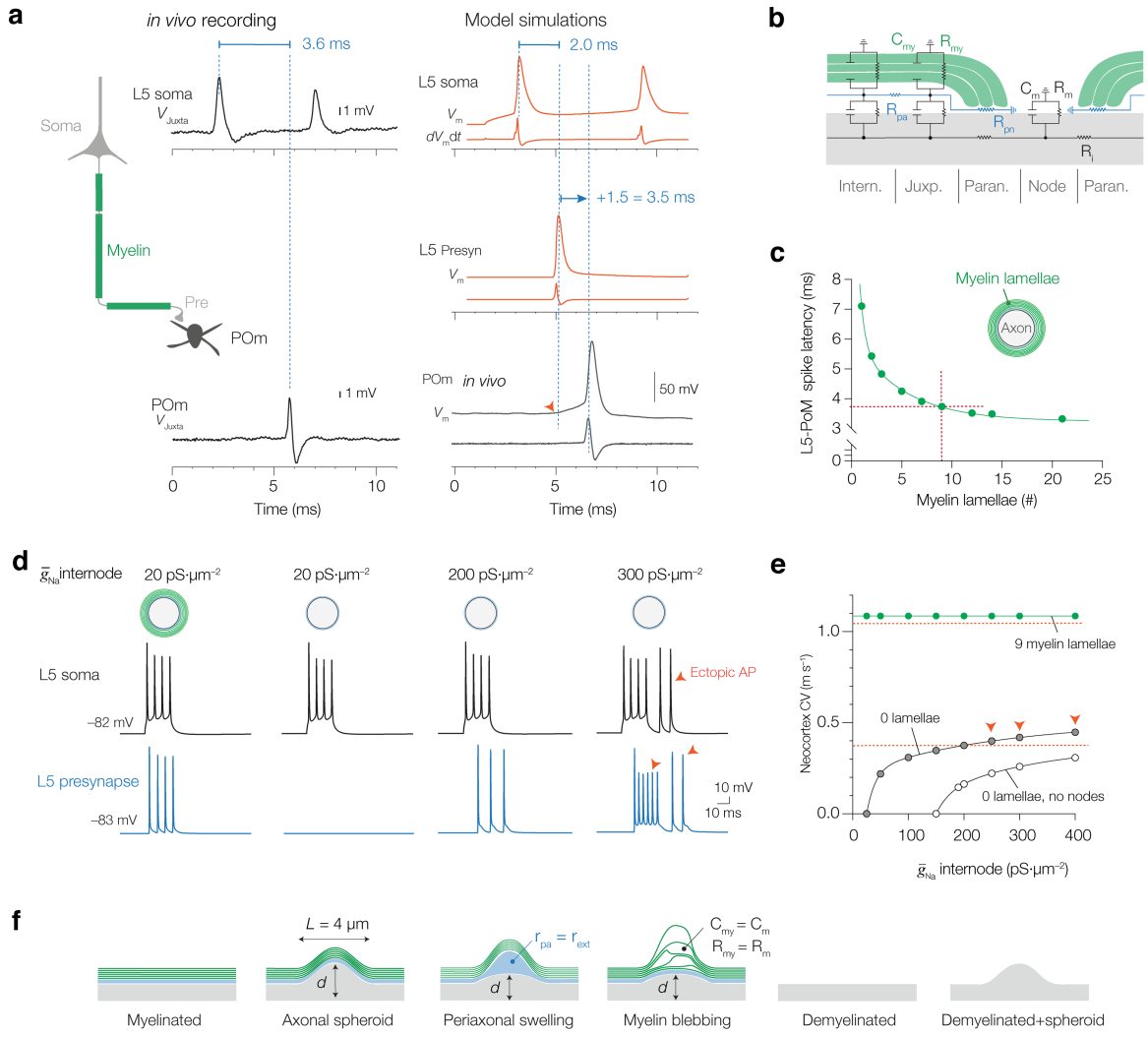

Supplementary Fig. 7 Experimentally constrained simulations of L5–POm delay and myelination

a *Left*, cartoon of L5–POm pathway with example of optotagged juxtacellular recordings from L5 or POm soma, aligned to the optogenetic stimulus onset, revealing a spike latency along monosynaptic pathways of 3.6 ms. *Right*, model simulations of voltage-time (*V-t*) and temporal derivative ($dV \cdot dt^{-1}$, orange traces) of L5 APs evoked by 20-ms current injections (1.7 nA) showing the first two spikes of a ~200 Hz burst cluster. The travel time from the soma to the giant synapse in control was 2.0 ms. L5–POm spike latencies were calculated by adding a nominal value of 1.5 ms. The constant of 1.5 ms was consistent with POm *in vivo* whole-cell recordings, revealing onset of EPSP to the peak dV/dt of the spike being on average 1.5 ms, consisted with published photo-evoked L5–POm EPSPs or spikes temporally separated by 1.5 ms (Ref. [27]).

b Double-cable electrical circuit diagram [3] used in the simulations consisting of nodal, paranodal, juxtaparanodal and internodal domains.

c Simulated L5-POm latencies reduce with increasing myelin lamellae number (reducing C_{my} proportionally). Red lines indicate a delay time of 3.5 ms with 9 myelin lamellae consistent with anatomical data [31,43,44].

d *Left*, example traces of burst transmission from soma to giant synapse in control simulations (9 lamellae). Removing myelin causes a complete spike failure, rescued by increasing sodium

peak conductance density (g_{Na}) in the internodal compartments. In the presence of nodal compartments, an increase of g_{Na} > 200 pS·μm^{-1} caused ectopic spikes (red arrow) initiated in the proximal region of the primary axon or demyelinated thalamic region. *Right*, removing NoR from the model abolished ectopic APs, increased spike initiation failure at the AIS and further slowed CV.

e CV in control (green), demyelinated with nodes (0 lamellae, grey circles) and demyelinated axon without nodes of Ranvier (open circles). Red arrows indicate model simulations with ectopic spikes. Red dashed line marks published CV for L5 pyramidal neuron axons in control (1.1 m·s^{-1}) and following cuprizone treatment (0.35 m·s^{-1}) [19,20]. A g_{Na} of 200 pS·μm^{-1} was selected for demyelinated models, below ectopic APs and consistent with experimentally measured CVs in demyelinated axons [19,20].

f Cartoon representations of the axonal and myelin swellings used in the simulations. Axonal spheroids were simulated in the morphologically realistic model at three internode locations in the neortex and one site in the white matter. We linearly increased the local model axon diameter (*d*) from 1.5 to 7 μm, over a length (*L*) of 4 μm. Periaxonal swellings were simulated by in addition lowering local r_{pa} to extracellular resistance r_{ext} values of 1×10^{-6} MΩ cm^{-1}. Myelin blebbing was simulated by setting C_{my} and R_{my} to neuronal membrane values. The largest conduction delay (~200 μs from soma to synapses) was caused by myelin blebbing.

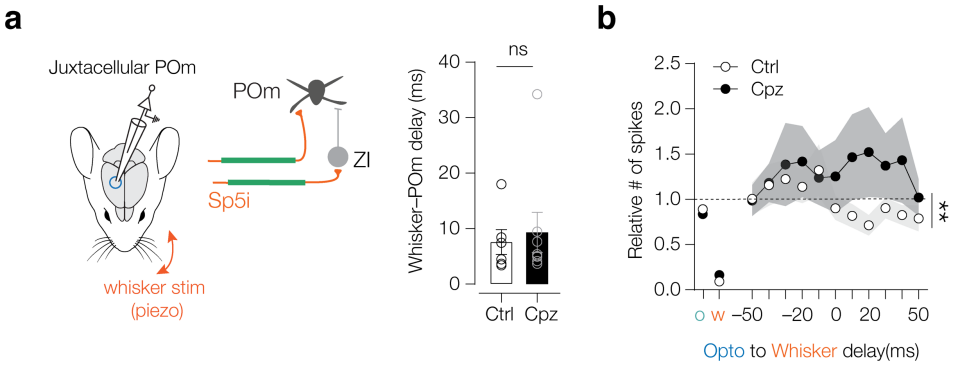

Supplementary Fig. 8 Demyelination of corticothalamic feedback alters the temporal encoding of whisker stimulation

a Invariant whisker-evoked delay in “early” responder neurons after demyelination. Mann-Whitney test P = 0.75. n = 6 neurons, N = 5 mice (Ctrl), n = 8 neurons, N = 7 mice (Cpz).

b Population average shows a preferential increase in spike numbers if the opto stim precedes the whisker stim for Ctrl but not for Cpz neurons. 2-way ANOVA P = 0.0082 treatment, P = 0.0007 delay, P = 0.79 interaction. Šídák's multiple comparisons test P > 0.05 for all comparisons. n = 15 neurons, N = 11 mice (Ctrl), n = 13 neurons, N = 7 mice (Cpz).

Supplementary Table 1. Antibody details

Antibody	Host	Dilution	Manufacturer	Cat. Nr.	RRID
Anti-Myelin Basic Protein	mouse	1:250	Covance	SMI-99P	AB_10120129
Anti-Red fluorescent protein	Chicken	1:1000	Synaptic Systems	409 006	AB_2725776
Anti-Red fluorescent protein	Guinea pig	1:1000	Synaptic Systems	390004	AB_2737052
Anti-Caspr	Rabbit	1:1000	Abcam	ab34151	AB_869934
Anti-Ankyrin G	Guinea pig	1:500	Synaptic Systems	386 004	AB_2725774
Streptavidin-Alexa488	/	1:500	Thermo Fischer	S11223	/
Streptavidin-Alexa594	/	1:500	Thermo Fischer	S11227	/
Anti-Rabbit Alexa405	Goat	1:1000	Thermo Fischer	A31556	AB_221605
Anti-mouse Alexa488	Goat	1:1000	Thermo Fischer	A10684	AB_2534064
Anti-guineapig Alexa488	Goat	1:1000	Thermo Fischer	A11073	AB_2534117
Anti-chicken Alexa594	Goat	1:1000	Thermo Fischer	A11042	AB_2534099
Anti-guineapig Alexa633	Goat	1:500	Thermo Fischer	A21105	AB_2535757
Anti-guineapig Alexa647	Goat	1:1000	Thermo Fischer	A21450	AB_2535867

Supplementary Movie 1
3D visualization of a stitched and fused light-sheet image showing the sparsely labelled L5 population (*magenta)* projecting to the spinal cord. One single axon was manually reconstructed from L5 continuing into the proximal spinal cord as well as an axon branch projecting to the POm (*white*), overlaid it with the imaged brain. Scale bar, 2 mm.

Supplementary Movie 2
Spatial profile of transaxonal (internodes) and transmembrane potentials (somatodendritic regions and noR) temporally aligned with the voltage-time plots for somatic (*black*) and giant terminal locations (*red*). A schematic version of the neuronal morphology is shown with myelin at approximate regions along the *x*-axis (*green*). For clarity, transmyelin and transfiber potentials are not shown. Movie shows one 20-ms duration high-frequency burst propagating along the control myelinated axon in rapid saltatory mode (1.93 $m \cdot s^{-1}$). Subsequent movie shows the example of cortical demyelination (slow continuous conduction, 0.35 $m \cdot s^{-1}$). Red arrows indicate demyelinated site and the propagation failure in the voltage-time plots of the terminal. Subsequent movie shows an expanded spatial scale revealing spike propagation block at the first noR. Final movie, axonal Na_v conductance density increased from 200 to 300 $pS \cdot \mu m^{-2}$ revealing ectopic APs starting from the second noR. Time resolution, 0.01 ms.